

N₂ Product Internal-State Distributions for the Steady-State Reactions of NO with H₂ and NH₃ on the Pt(100) Surface[†]

Alexander J. Hallock, Carl M. Matthews,[‡] Frank Balzer,[‡] and Richard N. Zare^{*,§}

Department of Chemistry, Stanford University, Stanford, California 94305

Received: March 5, 2001; In Final Form: May 16, 2001

The steady-state reaction of NO with H₂ and NH₃ on Pt(100) is investigated over a temperature range of 340–570 K, and the rotational and vibrational states of the N₂ product are probed by resonance enhanced multiphoton ionization. For NO + NH₃ the N₂ reaction product leaves the surface rotationally and vibrationally excited, whereas for NO + H₂ the desorbing N₂ is rotationally equilibrated with the surface and no vibrational excitation can be detected. We conclude that although these two surface reactions both yield N₂, the actual reaction mechanisms must be different.

Introduction

For reactions on well-defined surfaces knowledge of the internal energy distribution of one or all reaction products might give valuable hints to clarify transition states and verify models for potential energy surfaces. Hydrogen recombination reactions on various surfaces¹ provide examples of the information that can be gained from such studies. For heavier molecules, such as N₂, the situation is expected to be more complex but still can give insight into the shape of potential energy surfaces.²

In this study we examine the internal energy distribution of the N₂ product for two different precursor reactions on Pt(100): NO + NH₃ and NO + H₂. These catalytic reactions exhibit several notable features such as surface explosion,³ hysteresis in reaction rates, and kinetic oscillations.⁴ It is believed that for both systems the recombination of two nitrogen atoms on the Pt(100) surface leads to formation of N₂, N_a + N_a → N_{2,g} (with the subscript *a* for adsorbed species, and subscript *g* for gaseous). The N₂ subsequently desorbs from the surface. We show that the internal energy distributions of N₂ resulting from these two precursors are *not* the same, indicating that simple recombination models are inadequate. These differences might be interpreted as different transition states or different coverages for the two reactions.

Experimental Apparatus

In an ultrahigh vacuum (UHV) chamber^{5,6} a constant pressure of reactant gases is maintained. The chamber achieves a base pressure of 5×10^{-10} Torr by means of a liquid nitrogen trapped diffusion pump. A Pt(100) single crystal is fixed to a three-axis manipulator. This setup allows accurate positioning for the use of Auger, low-energy electron diffraction (LEED), and time-of-flight mass spectrometry (TOF MS). The sample can be heated to 1100 K by means of a filament located behind it. The sample can also be cooled to 170 K using liquid nitrogen. The temperature of the sample is monitored by a chromel–alumel thermocouple, spot-welded to its front face. The temperature of the Pt(100) single crystal is cycled, and product molecules

are detected both by a quadrupole mass spectrometer (QMS, Stanford Research Systems RGA200) and by resonance enhanced multiphoton ionization (REMPI) followed by time-of-flight (TOF) mass spectrometry. The latter scheme provides internal state identification. An advantage of our setup is that the TOF scans are run simultaneously with the QMS to ensure that the background gas pressures are approximately constant during the course of an experiment and to correct REMPI spectra with regard to small fluctuations in the reaction rates.

A Pt(100) surface adopts one of three arrangements depending on preparation conditions, temperature, and surface adsorbates: (1 × 1), hex, and hex-R0.7°. The hex-R0.7° face is the most stable configuration of a clean Pt(100) surface. The hex face is metastable and converts to the hex-R0.7° phase at temperatures above 1100 K. For both arrangements the surface atoms form a hexagonal structure, which is slightly buckled. The presence of adsorbates such as NO, CO, and O₂ revert the hex or hex-R0.7° to the bulk-terminated (1 × 1) configuration.⁹ These three arrangements can be easily distinguished by LEED.¹⁰ In our experiments only the hex- and (1 × 1)-face were observed, as expected from our preparation conditions.

The platinum surface was cleaned by sputtering with Ar⁺ ions at 1 keV while annealing at 900 K for 30 min. Auger spectra demonstrated that carbon is the most frequent contaminant. The carbon was removed by cooling the surface from 900 K (postannealing) to 470 K in 1.5×10^{-5} Torr of O₂ to oxidize the carbon on the surface to CO and CO₂. After this procedure, the surface was flashed to 900 K to desorb any remaining oxygen. Subsequent Auger scans verified that the carbon had been removed. In this way a clean Pt(100)-hex surface was prepared. We were able to reproduce the published LEED pattern of the hex reconstructed Pt(100) surface,¹⁰ usually with one predominant domain, and match previously published O₂, NO, and H₂ desorption.¹¹

To detect N₂ molecules in a state-selective manner, we employed a (2+1) REMPI scheme.^{12,13} Molecular nitrogen ions were produced by two-photon excitation from the X¹Σ⁺_g electronic ground state to the a¹Σ⁺_g Rydberg state, followed by one-photon ionization. We probed the (0,0) and (1,1) Q-branch lines because this branch has the highest intensity and is insensitive to molecular alignment. Tunable laser light around 202 nm was produced using a Nd:YAG pumped dye laser and two BBO crystals,⁶ guided into the UHV chamber, and focused

[†] Part of the special issue "Royce W. Murray Festschrift".

* Corresponding author. Fax: +1-650-725-0259. Email address: zare@stanford.edu.

[‡] Present address: Intel Corporation, Santa Clara, CA.

[§] Present address: Odense Universitet, Fysisk Institut, Campusvej 55, DK-5230 Odense M, Denmark.

about 2 cm in front of the surface. Nitrogen ions are generated at the entrance of a TOF tube and steered by various charged plates to a 40 mm multichannel plate array. The signal is acquired and sent to a computer via a digital oscilloscope. Experiments show that the laser power needs to be normalized with an exponent of 1.5, which is the typical behavior for a (2+1) REMPI transition showing geometric saturation.¹⁴ Peak heights are then corrected for nuclear spin statistics g_J , rotational degeneracy $(2J+1)$, and Bray–Hochstrasser line strength factors.¹⁵ If the distribution is characterized by a rotational temperature, the Boltzmann plot (the natural logarithm of corrected peak heights against rotational quantum number) is a straight line. We find that all data recorded are well described by linear Boltzmann plots, and therefore we report rotational temperatures.

We used high-purity gases for the experiments (H_2 99.999%, NO 99.5%, NH_3 99.999%). The major contaminants in the NO were N_2 (<3000 ppm) and CO_2 (<1000 ppm). A certain gas ratio was mixed in a stainless steel cylinder, and a total pressure of 3.7×10^{-7} Torr (uncorrected for differences in ion gauge sensitivity) was put into the chamber with the clean Pt(100) hex surface held at 900 K. Immediately afterward, the sample was cooled to 230 K. In this way we prepare a surface that is almost completely covered with NO . The ratios are chosen to maximize N_2 production. We used a 20% $\text{NO}/80\%$ H_2 mixture in the $\text{NO} + \text{H}_2$ case resulting in a sensitivity-corrected pressure as measured by ion gauge of 5.9×10^{-7} Torr, and 50% $\text{NO}/50\%$ NH_3 in the $\text{NO} + \text{NH}_3$ case resulting in 2.9×10^{-7} Torr.

The rotational excitation of the desorbing molecules is defined in terms of a mean rotational energy per molecule for each rotational distribution. In the case where a Boltzmann plot is linear, a characteristic rotational temperature can be assigned to the molecules. We found our distributions to be linear, although they can be prone to errors arising from noise in the high- J populations. To avoid this issue, the laser scan was made over a sufficiently large number of states, often out to $J = 24$ or further. During the experiments the surface temperature was cycled from 230 to 620 K (heating rate 0.5 K/s) and back again (cooling rate 1 K/s), while a constant pressure of adducts was maintained. To obtain rotational and vibrational distributions the temperature was selected and held constant while a REMPI spectrum was taken.

Results

A typical N_2 REMPI spectrum yields ion intensity as a function of dye fundamental wavelength. In Figure 1a the lower curve shows a typical REMPI spectrum for a mixture of NO and H_2 in the presence of the Pt(100) surface, probing N_2 in the vibrational ground state $v = 0$. The surface temperature was held at 273 K, i.e., no catalytic activity is present. The N_2 stems mainly from N_2 contamination of NO (approximately 3000 ppm) and from ambient gas in the chamber. Figure 1b presents the Boltzmann plot, from which a linear regression yields a rotational temperature of $T_{\text{rot}} = 293 \pm 25$ K. The upper curve in Figure 1a represents a REMPI spectrum for a surface temperature of 503 K, i.e., with catalytic activity present (circles in Figure 1b). After subtracting the background a rotational temperature can be extracted. Vibrationally excited states are only sparsely populated at room temperature; hence, reactive measurements for $v = 1$ or higher are essentially background free.

$\text{NO} + \text{NH}_3$. The primary reaction products for this reaction are N_2 and H_2O , as shown in Figure 2. Catalytic activity starts around 400 K, where the QMS shows a sharp rise in both the

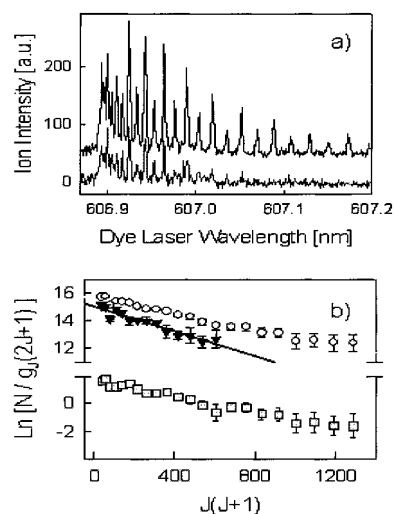


Figure 1. (a) The upper curve is a typical REMPI spectrum of N_2 from the $\text{NO} + \text{H}_2$ reaction with a surface temperature of 503 K. The lower curve is a spectrum of background N_2 in the chamber. (b) A Boltzmann plot of raw data (circles), the background showing a temperature of 293 ± 25 K (triangles), and the resulting subtraction (squares).

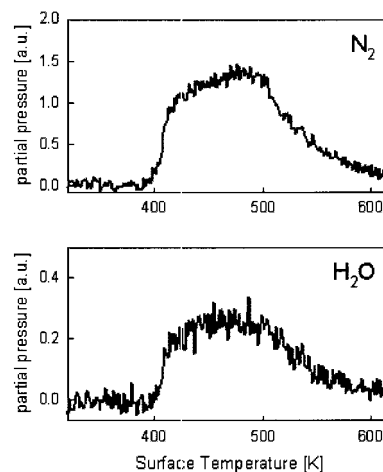


Figure 2. Rates of product formation for the quasi steady-state (heating rate 0.5 K/s) reaction $\text{NO} + \text{NH}_3$ on Pt(100) as a function of surface temperature. The traces represent NH mass 28 and 18, respectively.

N_2 signal at mass 28 and the H_2O signal at mass 18. As the surface temperature increases both signals remain on a high level up to 500 K, then drop and almost disappear around 600 K. This behavior is similar to previously observed temperature dependencies.¹⁶ The cooling curve is not shown in the figure, because the catalytic activity remains on a low level and we did not perform any REMPI measurements. This behavior is demonstrative of the reaction hysteresis. Product nitrogen is only formed in significant quantities while heating the surface over a certain temperature range in the presence of reactants. A typical spectrum took on the order of 2 h to acquire, during which time the gas concentrations were all monitored to ensure that the reaction was indeed steady-state.

In Figure 3a rotational temperature (circles) of desorbing N_2 molecules in $v = 0$ are presented as a function of surface temperature. Only between 416 and 485 K was it possible to find a stable reaction rate with enough product ion intensity to acquire a complete REMPI spectrum. The solid line denotes the rotational temperature that would result from a complete equilibration of the molecules with the surface. The rotational temperatures for $v = 0$ are far above thermal and increase with

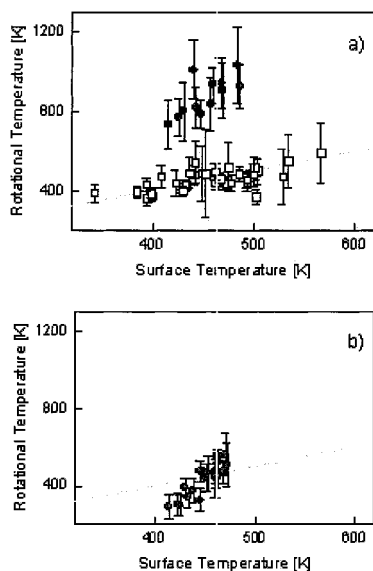


Figure 3. (a) Mean rotational energies as a function of surface temperature for desorbing N₂ molecules for the vibrational ground state $\nu = 0$. The white squares denote the reaction of H₂ with NO (1.18×10^{-7} Torr and 4.72×10^{-7} Torr respectively), the filled circles the reaction of NH₃ with NO (both 1.45×10^{-7} Torr). (b) Mean rotational energy for the reaction NH₃ with NO for $\nu = 1$. In both cases the gray line represents surface temperature (fully accommodated molecules).

surface temperature. Vibrational excitation of N₂ is clearly visible, too. From the population ratio $P(\nu=1)/P(\nu=0) \approx 0.2$ we estimate a vibrational temperature on the order of 2000 K. Rotational temperatures for $\nu = 1$ are presented in Figure 3b. We clearly see that the rotational temperature increases with surface temperature, but the energies are closer to thermal as compared to $\nu = 0$.

NO + H₂. For the NO + H₂ reaction three main reaction products occur, namely N₂, NH₃, and H₂O, as shown in Figure 4. N₂ production shows two peaks on the heating cycle. We clearly see competition between N₂ and NH₃ formation—ammonia production starts with a decrease in nitrogen signal and slows down as nitrogen slowly returns. Other investigators have also observed this change in selectivity.¹⁷

Rotational distributions of the N₂ product are taken for different surface temperatures ranging from 343 to 566 K. Although in Figure 4 catalytic activity is only observed between 400 and 600 K, this range can be extended to lower temperatures by starting the cooling cycle before the transition to the hex phase takes place; see the inset in Figure 4. Whereas catalytic activity is hindered during the heating cycle because of the high surface coverage with NO (see below), once the reaction started the surface coverage remains small and the reaction can proceed even at low temperatures.

The reaction exhibits hysteresis over the entire temperature range investigated. We wanted to see if N₂ production in the cooling direction looked rotationally different than N₂ production when heating. N₂ was produced in barely detectable amounts which showed up as a broad peak around 150 K. The extremely small amount of product produced lead to noisy spectra. We conclude that there is no large change from a thermal distribution so the formation mechanism might be the same.

The squares in Figure 3a show the temperature dependence of the rotational temperature of N₂. In contrast to N₂ from NO + NH₃ the molecules seem to be rotationally accommodated with the surface. After extensive searching for both the $\nu = 1$ and $\nu = 2$ band heads, we conclude if vibrational excitation exists, it is below our ability to detect it. We estimate that this

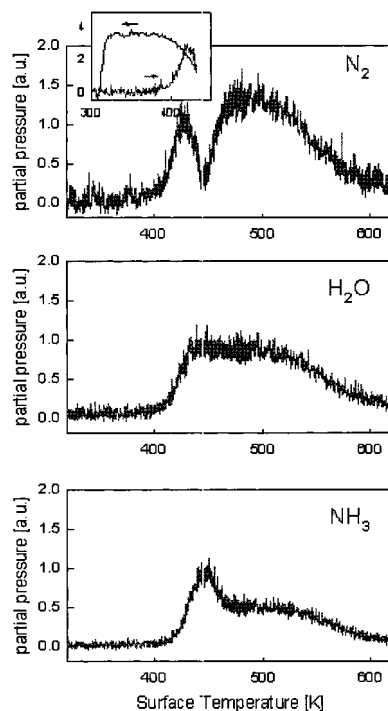


Figure 4. Same as Figure 2, but for the reaction NO + H₂. The traces represent mass 28, 18, and 17, respectively. The insert demonstrates how to get catalytic activity for surface temperatures lower than 400 K by cooling before the surface phase transition to the Pt hex phase takes place.

would make the vibrational temperature well below 1000 K. This result is surprising because a simple recombination of N atoms to form N₂ would be expected to produce much vibrationally excited molecules.

Discussion

Previous experiments on the NO + H₂ and NO + NH₃ reactions have revealed largely similar mechanisms.^{4,18} In contrast, our study of the internal state distributions of the resulting N₂ product reveals quite different behavior. Indeed, this work establishes the value of being able to observe in detail the escaping products of a well-defined surface reaction.

Two key steps dictate the temperature dependence of the reaction rates: NO dissociation and the $(1 \times 1) \leftrightarrow$ hex phase transition. Up to 350–400 K, a high NO coverage stabilizes the (1×1) Pt(100) surface. NO dissociation, which occurs above 380 K,¹⁹ is the rate-limiting step for the reactions. The reactivity of the NO covered surface is low, because for NO dissociation a free adsorption site is necessary. Free adsorption sites occur only above 400 K for which temperature desorption of adsorbed NO and NH₃ or H₂ takes place. Consequently, the reactions can only start above this temperature. The reaction product water is weakly bound to the surface and desorbs immediately after formation.²⁰ The only important pathway for forming N₂ seems to be the recombination of N atoms on the surface.¹⁸ Atomic N has a finite residence time on the surface.²¹ Additional free adsorption sites are created via desorption of reaction products, and the reaction proceeds rapidly. The surface coverage with NO decreases, whereas the coverage with intermediates like NH_x ($x=1-3$) (known from work function measurements) increases. Between 500 and 600 K the phase transition from the (1×1) to the hex surface takes place. The hex phase is not active in NO dissociation³ with the exception of edge defects.²² Consequently the reactivity ceases.

N_2 itself does not adsorb on the Pt(100) face at room temperature.²¹ King et al.^{23,24} demonstrated that the sticking probability for N_2 on Pt(100) is zero for translational energies up to 3 eV, and they concluded that recombinative desorption on Pt(100) proceeds directly through a late barrier, without trapping and equilibration to the surface temperature. This mechanism results in vibrationally excited gaseous N_2 . In agreement with this mechanism, Foner et al.²⁵ found evidence for excitation up to $v = 9$ for N_2 recombination after NH_3 dissociative adsorption on polycrystalline platinum.

Vibrationally excited N_2 has been observed in recombination reaction on several other metals like sulfur covered polycrystalline iron,²⁶ on Cu(111),²⁷ Ru(001),²⁸ and Ag(111).²⁹ In each of these systems, the vibrational temperatures are much higher than the surface temperature. The transition states of these reactions must feature atoms that are separated by distances greater than equilibrium bond length. Furthermore, the very large vibrational spacing in the N_2 molecule (approximately 2360 cm^{-1}) precludes rapid equilibration with the surface.

Because the N atoms are thought to recombine for both precursors as they might do in a simple recombination scenario we expected to observe vibrationally excited N_2 product in the $NO + H_2$ and the $NO + NH_3$ reactions. We also expected to observe rotationally excited N_2 products because of the large nitrogen–nitrogen distance in the transition state. For the reaction between NO and NH_3 these expectation were met for this case, but for $NO + H_2$ surprisingly they were not. Instead the N_2 seems to be completely equilibrated (at least rotationally) with the surface. We conclude that two different mechanisms are operative but presently we can only speculate what might be the reasons for this behavior. It is obvious that the source of N atoms on the Pt surface can be different for both systems. For $NO + H_2$ the N atoms stem solely from dissociation of NO, but for $NO + NH_3$ two possible origins exist. Imbihl et al.¹⁶ studied the $NO + NH_3$ reaction via isotopically labeled adducts and demonstrated that the desorbing N_2 is produced entirely from NO only for temperatures above 500 K. For lower temperatures, N_2 stems either from dissociated NH_3 alone, or from NO and NH_3 . For this reaction we only could take REMPI spectra to a surface temperature of 485 K due to decreasing N_2 production and increasing backgrounds. This means we probe N_2 that is made of at least one nitrogen from dissociated NH_3 , not entirely from NO. Consequently, the possibility exists that the N_2 we observe comes from another reaction like $N_a + NO_a \rightarrow N_{2,g} + O_a$, which would account for the different internal state distribution. For N_2 formation during NO reduction at Pd(110)³⁰ these two N_2 forming reactions have been identified to lead to different angular distributions of desorbing N_2 and to different state distributions, although on Pt(335) $N_a + NO_a$ has not been seen.³¹ Another possibility could be that different coverages of the surface with reaction adducts or intermediates as NH_x , structural surface defects especially in the vicinity of adduct islands or the formation of complexes like $NO_a-NH_{x,a}$ ¹⁶ influence the height of the barrier to the $N_a + N_a$ recombination. This second possibility cannot be ruled out but seems to be less attractive than the first.

Conclusions

Our study shows that the $NO + H_2$ and $NO + NH_3$ reactions behave in similar fashions but they reach their respective final states through different intermediates. We base this conclusion on the different distributions of energies in the N_2 product. Traditional methods for probing surface chemistry are blind to this type of effect. The precise mechanism accounting for the different intermediates still needs clarification, but the measurement of N_2 product internal energy distributions for $NO + H_2$ and $NO + NH_3$ on Pt(100) shows unequivocally the need for further study of these reaction systems.

Acknowledgment. C.M.M. thanks the Hertz-Foundation, and F.B. thanks the Deutsche Forschungsgemeinschaft (Ba 1858/1-1 and Ba 1858/1-2) for financial support. This study was supported by the U.S. National Science Foundation under Grant. CHE-9900305.

References and Notes

- (1) Bent, S. F.; Michelsen, H. A.; Zare, R. N. *Laser Spectroscopy and Photochemistry on Metal Surfaces*; World Scientific: Singapore, 1995.
- (2) Hodgson, A. *Prog. Surf. Sci.* **2000**, *1*, 63.
- (3) Lesley, M. W.; Schmidt, L. D. *Surf. Sci.* **1985**, *155*, 215.
- (4) Lombardo, S. J.; Fink, T.; Imbihl, R. *J. Chem. Phys.* **1993**, *98*, 5526.
- (5) Ellison, M. D.; Matthews, C. M.; Zare, R. N. *J. Chem. Phys.* **2000**, *112*, 1975.
- (6) Matthews, C. M.; Balzer, F.; Hallock, A. J.; Ellison, M. D.; Zare, R. N. *Surf. Sci.* **2000**, *12*, 460.
- (7) Kuhnke, K.; Kern, K.; Comsa, G.; Moritz, W. *Phys. Rev. B* **1992**, *45*, 14388.
- (8) Ritz, G.; Schmid, M.; Varga, P.; Borg, A.; Ronning, M. *Phys. Rev. B* **1997**, *56*, 10518.
- (9) Norton, P. R.; Davies, J. A.; Creber, D. K.; Sitter, C. W.; Jackman, T. E. *Surf. Sci.* **1981**, *108*, 205.
- (10) Hagstrom, S.; Lyon, H. B.; Somorjai, G. A. *Phys. Rev. Lett.* **1965**, *15*, 491.
- (11) Norton, P. R.; Griffiths, K.; Bindner, P. E. *Surf. Sci.* **1984**, *138*, 125.
- (12) Lykke, K. R.; Kay, B. D. *J. Chem. Phys.* **1991**, *95*, 2252.
- (13) Hanisco, T. F.; Kummel, A. C. *J. Chem. Phys.* **1991**, *95*, 8565.
- (14) Zakheim, D. S.; Johnson, P. M. *Chem. Phys.* **1980**, *46*, 263.
- (15) Bray, R. G.; Hochstrasser, R. M. *Mol. Phys.* **1976**, *31*, 1199.
- (16) Lombardo, S. J.; Esch, F.; Imbihl, R. *Surf. Sci. Lett.* **1992**, *271*, L367.
- (17) Madden, H. H.; Imbihl, R. *Appl. Surf. Sci.* **1991**, *48/49*, 130.
- (18) Slinko, M.; Fink, T.; Löher, T.; Madden, H. H.; Lombardo, S. J.; Imbihl, R.; Ertl, G. *Surf. Sci.* **1992**, *264*, 157.
- (19) Fink, T.; Dath, J. P.; Bassett, M. R.; Imbihl, R.; Ertl, G. *Surf. Sci.* **1991**, *245*, 96.
- (20) Ibach, H.; Lehwald, S. *Surf. Sci.* **1980**, *91*, 187.
- (21) Schwaha, K.; Bechthold, E. *Surf. Sci.* **1977**, *66*, 383.
- (22) Miners, J. H.; Gardner, P. *J. Phys. Chem. B* **2000**, *104*, 10265.
- (23) King, D. A. *Faraday Discuss.* **1993**, *96*, 79.
- (24) Bradley, J. M.; Hopkinson, A.; King, D. A. *J. Phys. Chem.* **1995**, *99*, 17032.
- (25) Foner, S. N.; Hudson, R. L. *J. Chem. Phys.* **1984**, *80*, 518.
- (26) Thorman, R. P.; Bernasek, S. L. *J. Chem. Phys.* **1981**, *74*, 6498.
- (27) Murphy, M. J.; Skelly, J. F.; Hodgson, A. *J. Chem. Phys.* **1998**, *109*, 3619.
- (28) Murphy, M. J.; Skelly, J. F.; Hodgson, A.; Hammer, B. *J. Chem. Phys.* **1999**, *110*, 6954.
- (29) Carter, R. N.; Murphy, M. J.; Hodgson, A. *Surf. Sci.* **1997**, *387*, 102.
- (30) Haq, S.; Hodgson, A. *Surf. Sci.* **2000**, *463*, 1.
- (31) Wang, H.; Tobin, R. G.; DiMaggio, C. L.; Fisher, G. B.; Lambert, D. K. *J. Chem. Phys.* **1997**, *107*, 9569.